Update on the use of a simulation-based approach to evaluate plausible levels of recruitment into the Pacific Coast Feeding Group of gray whales

Lang, A.R., and Martien, K. K.
Protected Resources Division, Southwest Fisheries Science Center, La Jolla, CA 92037

ABSTRACT

Previous genetic comparisons of the Pacific Coast Feeding Group (PCFG) of gray whales with whales feeding north of the Aleutians have shown significant levels of mitochondrial differentiation. The magnitude of the differentiation, along with the relatively high levels of genetic diversity identified within the PCFG, have raised questions about how much immigration into the group could occur before the signal of mtDNA differentiation is erased. Here we use a simulation-based approach to evaluate the range of plausible levels of immigration into the PCFG that could be occurring. The simulations incorporate annual immigration ranging from between 0 and 16 animals per year (once the larger ENP population reaches K), and simulations both with and without a pulse of +20 immigrants over two years are included. Results suggest that under the scenarios tested, current immigration into the PCFG of one migrant per year or less would produce levels of genetic diversity and differentiation that are inconsistent with the empirical data. The simulations were less informative with regard to placing an upper limit on the number of animals per year which could be immigrating into the PCFG, although comparison of F_{ST} and χ^2 (per degree of freedom) values between the simulated and empirical data suggests that immigration higher than 8 animals per year is unlikely. Comparisons between the observed and simulated values for the number of haplotypes, F_{ST}, and χ^2 (per df), which were the most informative measures, suggest that immigration of approximately 4 animals per year is most plausible.

INTRODUCTION

Genetic comparisons of samples collected from gray whales considered to be part of the Pacific Coast Feeding Group (PCFG) with those from animals that feed north of the Aleutians have revealed small but significant levels of mtDNA differentiation but no nuclear differentiation (Lang *et al.* 2011). In addition, a relatively large number of mtDNA haplotypes were identified within the PCFG (n=23 haplotypes, Lang *et al.* 2011), which is estimated to contain ~200 animals (IWC 2011). Analysis of photo-identification data indicates that on average, 10 animals per year were recruited[1] into the PCFG between 2004 and 2008, with larger numbers of recruits identified between 2000 and 2002 (IWC 2011). These recruits could be internal (i.e., calves born to PCFG mothers) or external (animals that previously fed north of the Aleutians and subsequently immigrated into the PCFG). An average of three calves per year were identified in the PCFG between 1998 and 2008 (Calambokidis *et al.* 2010), and it is presumed that at least half of the calves born each year may not have been identified as such (IWC 2011). Based on those assumptions, an estimated four animals per year may have recruited into the PCFG from northern feeding area(s) between 2004 and 2008, and a pulse of higher immigration may have occurred between 1999 and 2002, potentially in response to the increase in gray whale mortality that occurred in 1999 and 2000.

The results of these genetic and photo-id studies of the PCFG have raised questions about how much external recruitment into the PCFG could occur while still maintaining the observed level of mtDNA differentiation between the PCFG and animals feeding north of the Aleutians. The use of a simulation-based approach has the potential to provide information relevant to this question. As part of a previous IWC exercise (the Testing of Spatial Structure Methods, or TOSSM, project), simulated genetic datasets representing different population structure archetypes were created for performance testing of different analytical methods (Martien *et al.* 2009). The demographic parameters underlying the dataset generation model were based on the vital rates of

---

[1] Here a 'recruit' is defined as an individual first photographed in the PCFG seasonal range (within the area spanning 41-52°N and between June 1 and November 30) in a given year and resighted within the seasonal PCFG range in at least one subsequent year.

eastern gray whales (Martien *et al.* 2004, Martien 2006). In discussions with the IWC Stock Definition subcommittee, it was agreed that the TOSSM dataset generation model could be useful in creating simulated datasets that would allow the plausibility of different hypotheses (e.g., different immigration rates into the PCFG) to be evaluated.

METHODS

Rmetasim

Simulated datasets were produced using the *rmetasim* package (version 1.1.05, Strand 2002) as run in the R statistical environment (R 2.14.1). *Rmetasim* performs individual-based population genetic simulations utilizing stage-based matrix population models. The transition probabilities in the matrices are used to randomly assign births, stage transitions, and deaths of individuals over time. Density dependent growth is implemented by the linear interpolation between matrices representing survival and reproduction rates at carrying capacity (K) and at zero population density (ZPD). A pre-birth pulse model is used, such that at the end of each simulation year, the youngest animals in the population are one year old.

Stage-based matrices

As previously mentioned, vital rate estimates for eastern Pacific gray whales (as described in Martien *et al.* 2004, Martien 2006) were used to parameterize stage-based matrices for the TOSSM exercise. Since the construction of these matrices, additional information has become available on the life history of gray whales. This new information was utilized to update the stage-based matrices from TOSSM, and when possible the vital rates used in constructing the new matrices were chosen to be the same as those utilized in the IWC's Implementation Review of gray whales. The following changes were made:

1) Adult survival rate was increased to the median estimate from Punt & Wade 2010 (S_A=0.982)
2) A separate term for calf survival rate (set to S_c=0.732, the median estimate in Punt & Wade 2010) was utilized. In the previous matrices, calf survival was the same as juvenile survival.
3) The median estimate from Punt & Wade 2010 was utilized for the rate of increase at ZPD (λ =1.063)
4) The age of first reproduction (AFR) was increased to 7 years at ZPD based on the Bradford *et al.* 2010 review.
5) A third juvenile stage was added to provide better control of AFR.

In addition, three identical adult stages for each sex were included in the new matrices. In contrast, the matrices used in the TOSSM project included a single adult male stage and separate fertile and lactating stages for adult females. This change was implemented for two reasons. First, it allowed for better control of generation time and greatly reduced the proportion of individuals in the simulations that lived to unrealistic ages under the increased adult survival rate. Secondly, it reduced the number of multiple births by the same female in a given year. In *rmetasim*, the fertility term represents the mean number of calves produced per female based on a Poisson distribution (Strand 2002). This results in some females producing more than one calf per year. Eliminating the separate fertile and lactating stages allowed us to reduce the fertility term (since it was applied to all adult females, not just a subset in the lactating stage), thereby reducing the number of multiple births (Table 1). However, this change also eliminated the minimum two-year calving interval that had been enforced in the TOSSM matrices. As such, under the new matrices some females in the simulation will give birth in consecutive years (Table 2).

Given the number of changes implemented in the new matrices, we ran the simulations using both the updated nine-stage matrices as well as the original five-stage matrices (as described in Martien 2006) utilized in the TOSSM exercise. The vital rates used to construct the original matrices and those utilized in the updated 9-stage matrices are detailed in Table 3. The parameter for juvenile survival rate was not derived from the literature but was calculated from the matrices to produce the desired value of lambda. The

Maximum Sustainable Yield Rate (MSYR) calculated from the 9-stage matrices is ~3.3%, while MSYR for the 5-stage TOSSM matrices is ~3.6%.

These vital rates were used to construct stage-based matrices representing the demography of the population near carrying capacity (K) and near zero population density (ZPD). Transition probabilities were calculated according to Caswell (2001) and the resulting matrices are shown in Table 4.

Population Trajectories

Dataset generation followed the steps outlined in Martien 2006, with the exception that coalescent datasets were generated using FastSimcoal (Excoffier and Foll, 2011) rather than SimCoal 2.1.2 (Laval and Excoffier 2004) to establish the effective size (Ne). In all scenarios, a single population was simulated in *rmetasim* for 4000 years to provide datasets representing the equilibrium population. This time period was shown to be sufficient for reaching equilibrium in a similar exercise for bowhead whales (Archer *et al.* 2010), that have a markedly longer generation time.

The mutation parameter incorporated in the simulations was adjusted to produce genetic diversity levels (as measured by the number of haplotypes and the haplotypic diversity) that are similar to the values observed for the "North" strata in the Lang *et al.* 2011 study. A range of mutation parameters were explored before setting the mutation parameter to 3.8×10^{-3} per generation, which produced measures of genetic diversity that were the most consistent with the observed data.

Carrying capacity (K) for the larger ENP population of gray whales was set to 20,000 animals, similar to the most recent abundance estimate (19,126 animals in 2006/2007; Laake *et al.* 2009). Carrying capacity for the PCFG was set to 200 in accordance with the estimated abundance of 194 animals in 2008 (Annex F, IWC 2011).

For all population trajectories, depletion due to commercial whaling was simulated as having occurred between 1846 and 1930. Attempts were made to utilize the catch history (Annex E, IWC 2011) with a multiplier to produce the desired level of depletion in 1930 (10% of K). However, when this modification was incorporated it resulted in a high number of simulation runs that failed due to the simulated population(s) going extinct. As such, the depletion per year was set to a constant proportion of K, such that the population was depleted by 7.1% of K in each year for the duration of the simulated whaling period. This level of depletion allowed the population to reach the desired level (0.10 of K, or ~2000 animals) by 1930. Examples of the population trajectories produced are shown in Figure 5.

Given that little is known about the origin of the PCFG, two different population histories were simulated. The first scenario ("post-whaling split") assumes that the PCFG split from the larger ENP population following depletion. After reaching equilibrium a single population was projected forward through the 1846-1930 whaling period with depletion occurring as described above. In 1930, 20 animals (10% of K_{PCFG}) were split from the larger population to represent the PCFG. The two populations were then allowed to increase until reaching K. *Rmetasim* employs a "hard ceiling" to restrict population growth to K, such that individuals are killed off randomly after reaching levels >10% higher than K.

The second scenario ("pre-whaling split") assumes that the PCFG split from the larger ENP gray whale population prior to the depletion of gray whales due to commercial whaling. In this scenario, the equilibrium population was split into two feeding groups to represent the northern feeding ground (K_{ENP}=20,000) and the PCFG (K_{PCFG} = 200). The split was presumed to occur at the start of the Little Ice Age (considered here to be at 1540), a period in which it seems plausible that ice conditions would have been favorable for gray whales to begin using more southern feeding grounds. Both populations were projected forward until 1846, when the depletion due to commercial whaling was simulated as described above. After reaching 1930, the simulated depletion ceased and the two populations were allowed to grow until reaching K.

Immigration rates ranging from 0 to 0.0008 were simulated. These migration rates correspond to the immigration of between 0 and 16 animals per year into the PCFG from the larger ENP population once it has reached K (Figure 6). In addition, each population history and migration rate combination was also simulated with a migration "pulse" of 20 individuals over two years. This pulse is reflected in the abundance of the PCFG in 2000 and in 2001. Examples of abundance trajectories for the PCFG under the different immigration scenarios are shown in Figure 7.

Additional simulations were performed in which the value of K_{PCFG} was increased from 200 to between 500 and 5000. These simulations incorporated a post-whaling split of the PCFG from the larger ENP, with the pulse migration of +20 animals over two years but no annual immigration into the PCFG. As in the "post-whaling split" scenarios described above, the split of the PCFG from the larger ENP was modeled such that the number of animals colonizing the PCFG in 1930 was 10% of K.

A final set of simulations were performed that incorporated a more recent split (between 1940 and 1990) of the PCFG from the larger ENP population. The number of animals splitting off to form the PCFG in a given year was derived by taking an average (over ten replicates) of the simulated abundance of the PCFG in each year when the abundance trajectories were modeled under the scenario of a post-whaling split of the PCFG in 1930 with no annual immigration.

A list of scenarios that have been simulated to date is included in Table 7. Of note, the simulations incorporating a pre-whaling split of the PCFG from the larger ENP are in progress and have not yet been completed.

Sampling and Genetic Analyses:

To generate the simulated dataset, the number of simulated animals sampled per year was set to match the number of animals sampled per year and per stratum in the Lang *et al*. (2011) study (Table 8). In the empirical study, some animals were sampled multiple times, and only one sample per individual was retained for the data analysis. For the simulated sampling, the year of sampling for such individuals was assigned as the first year that the animal was sampled. A total of 103 samples were collected from simulated ENP individuals and 71 samples were collected from simulated PCFG individuals.

These sampled individuals were used to generate summary statistics for each group. Genetic diversity was characterized by the number of mtDNA haplotypes, the mtDNA haplotype diversity, and the mtDNA nucleotide diversity. Differentiation between the two simulated groups was measured using F_{ST}, χ^2 (per degree of freedom), and ϕ_{ST}. The summary statistics generated from the simulated datasets were then compared to the observed summary statistics generated for the PCFG and the North strata in Lang *et al.* 2011.

To further evaluate how well the shape of the haplotype frequency distribution for the simulated ENP population matched the shape of the distribution for the North stratum in the empirical data, a χ^2 test was used to compare the two haplotype frequency distributions, and the number of significant tests ($p<0.05$) was calculated. In addition, the frequency of the most common haplotype in each replicate simulation was calculated and compared to the frequency of the most common haplotype in the empirical data for the North stratum. Given that the mtDNA summary statistics produced for the simulated ENP population under all scenarios was similar, these tests were only conducted using the data for the simulated ENP population produced under the model with a post-whaling split with pulse migration but no annual immigration.

In addition to showing the proportion of simulations that had higher and lower values for each statistic than the values generated from the empirical data, we used interpolation to calculate the "crossover point" at which the 50% probability (median) was reached (i.e. the point at which the proportion of simulated runs had values higher than the observed reached 50%). For the number of haplotypes, the crossover point was

calculated as the point at which the lines representing the proportion greater than and the proportion less than crossed (as for the other statistics), but because some simulation replicates had values equal to (rather than less than or greater than) the observed value, this point was slightly lower than the 50% probability.

RESULTS

Although the goal is to produce 500 replicates of each scenario, currently only 100 replicates of each scenario are complete and are utilized in the results shown here.

Comparison of simulated and observed data for ENP

Table 9 includes a summary of the number of haplotypes, haplotypic diversity and nucleotide diversity for the simulated ENP population for the model incorporating the 9-stage matrices with a post-whaling split and pulse immigration. Results were similar under all scenarios tested (data not shown). Overall, median values for both the haplotypic diversity and the number of haplotypes were similar among the simulated and empirical datasets. The haplotypic diversity values generated in the simulated data were slightly lower than that in the observed data, with median values for the simulated data ranging from 0.948 to 0.950 (as compared to the observed haplotypic diversity of 0.952) and with 52-64% of replicates under the different immigration scenarios having lower haplotypic diversity than found in the empirical data. In contrast, the median number of haplotypes generated in the simulated datasets (33 to 34 haplotypes) was slightly higher than that found in the observed data (32 haplotypes). Between 62 and 75% of replicates for the different immigration scenarios generated values higher than the number identified in the empirical dataset. Although the nucleotide diversity calculated from the empirical data fell within the 90% range of the simulated values, nucleotide diversity in the simulated data was higher than that found in the observed data.

To evaluate whether the shape of our simulated haplotype distributions matched the shape of the observed distribution, we used a χ^2 test to compare the observed (North stratum) versus the simulated haplotype frequency distributions for the ENP population. The χ^2 test evaluates whether the haplotype distributions representing the empirical and simulated data could have been generated by random sampling of a single population. The χ^2 test is particularly sensitive to the frequencies of the most common haplotypes, as those haplotypes are the most likely to be represented in the random draws that represent immigration events. In our comparison, 12% of tests showed significant ($p<0.05$) differences (Figure 10), suggesting that the shape of the observed and simulated distributions were similar in most cases. We also compared the frequency of the most common haplotype in the empirical data with the frequency of the most common haplotype in the simulations. We found that the frequency of the most common haplotype was higher than that found in the empirical data for 47% of the simulation replicates. This finding is consistent with the expectation that if two samples are drawn from the same distribution, the frequency of most common haplotype would be expected to be greater in one sample than the other 50% of the time.

Comparison of simulated and observed data for the PCFG

Figure 11 shows a graphical representation of the proportion of simulated values for each statistic that are lower (shown in black) or higher (shown in gray) than the observed value generated from the empirical data for one of the scenarios tested (post-whaling split with pulse immigration, nine-stage matrices). Summaries of the number of mtDNA haplotypes (Table 12), mtDNA haplotype diversity (Table 13), mtDNA nucleotide diversity (Table 14), F_{ST} (Table 15), ϕ_{ST} (Table 16), and χ^2/df (Table 17) produced by the simulations under all completed scenarios are shown below.

With regard to comparisons between the observed and simulated data, the statistics based on haplotype frequencies (haplotypic diversity, $F_{ST,}$ and χ^2/df) and haplotype numbers were the most informative. For all four of these statistics, scenarios based on annual immigration of one animal or less per year (at K) produced values that were inconsistent with the empirical data. The comparisons were less informative with regard to the highest level of immigration that could be occurring, although comparison of F_{ST} and χ^2/df values suggested that levels of immigration including > 8 animals/year (along with the pulse immigration) would produce values inconsistent with those produced by the empirical data.

Similar to the pattern seen in comparison of the observed and simulated data for the larger ENP population, the nucleotide diversity identified among the simulated datasets was higher than that seen in the empirical data. In the ϕ_{ST} comparisons, the value generated in the empirical comparison was more consistent with the lower range of values for annual immigration and indicated that more than 8 immigrants per year into the PCFG would produce values of ϕ_{ST} lower than that observed. Caution should be applied when interpreting this pattern, however, given the lower nucleotide diversities identified in the observed data when compared to the simulated datasets.

Table 18 shows the results of simulations evaluating scenarios in which the PCFG splits from the larger ENP population between 1940 and 1990. The results shown suggest that for no annual immigration into the PCFG to be plausible, the PCFG would have had to split from the larger population after 1950.

Table 19 shows the results of simulations evaluating scenarios in which the carrying capacity for the PCFG was set to between 500 and 5000. The results indicate that the carrying capacity for the PCFG would need to be higher than 500 animals for the simulated results to be consistent with the empirical data under a scenario of no annual immigration. Examples of the abundance trajectory of the PCFG for the K values tested are shown in Table 20. For all K values simulated, the abundance of the PCFG was close to carrying capacity by 2010 (Table 21).

DISCUSSION:

Comparison of the simulated and empirical datasets for the larger ENP population suggests that the simulations represent the empirical data reasonably well with regard to the number of haplotypes and their distribution. Although the simulations predict that we would find slightly higher number of haplotypes and a slightly lower haplotypic diversity than is present in the empirical data, the differences are small and the χ^2 test suggests that the two samples would be interpreted as being drawn from the same population in the majority (88%) of cases. The results of these comparisons suggest that similar frequency-based comparisons of the simulated and empirical data representing the PCFG should be informative.

The level of nucleotide diversity in the simulated data representing the larger ENP population is higher than that found in the empirical data, indicating that there are some aspects of the population's history that are not being captured by the simulations. It is likely that the gray whales in the North Pacific have experienced numerous fluctuations in abundance due to changing ice conditions in the past, and historic K may have been substantially larger than we have simulated here (e.g., Alter *et al*. 2007). Our simulations incorporate only a simplified version of the recent history of gray whales, and our results suggest that the statistics relying on nucleotide differences (e.g., nucleotide diversity and ϕ_{ST}) may be more sensitive to violations of our assumptions about past (pre-commercial whaling) population size and equilibrium. As such, the results derived from the comparisons of nucleotide diversity and ϕ_{ST} warrant further investigation and should be interpreted with caution.

The comparison of frequency-based statistics between the simulated and empirical datasets representing the PCFG suggests that annual immigration into the PCFG is likely to be higher than 1 immigrant per year under the scenarios tested. The simulations were less informative with regard to the upper bound on annual immigration that could be occurring. Although the F_{ST} and χ^2/df comparisons indicated that immigration of >8 animals/year would be inconsistent with the empirical data, the proportion of simulations with higher than the observed values for the number of haplotypes and the haplotypic diversity never exceeded 84% and 63%, respectively. For all four statistics, the proportion of simulations with higher (for the number of haplotypes and haplotypic diversity) or lower (for F_{ST} and χ^2/df) values than the observed appears to level off at the higher (8 -10 or more per year) levels of immigration. This pattern is particularly evident in the comparisons utilizing haplotypic diversity, where the proportion of simulations with higher or lower values than the observed levels off at ~50% for immigration of 8 or more animals per year. Haplotypic diversity is calculated based on the sum of squared allele frequencies. Given that relationship, as the number of haplotypes in a population increases, the addition of another haplotype, particularly one found in low frequencies as would be expected to be brought in by an immigrant, has little impact on diversity. As such, this statistic, and to a lesser extent the others, appear to have limited power to differentiate between the higher levels of immigration.

Although these statistics were limited in their ability to distinguish an absolute upper bound on how much immigration could be occurring, the calculation of the number of immigrants per year which corresponds to the "crossing point" provides some information on what the most plausible values of immigration could be (Table 22). The estimated number of migrants ranged from ~2 to 8 for the scenarios with pulse immigration under the updated matrices. For the reasons discussed above, the calculations based on ϕ_{ST} and haplotypic diversity may not provide the best estimates. Comparisons between the observed and simulated values for the number of haplotypes, F_{ST}, and χ^2/df, suggest that immigration of approximately 4 animals per year is most plausible. If the current abundance of the PCFG is approximately 200 animals, this represents immigration of ~ 2% per year. Of note, this estimate does not include the +20 animals which were simulated to immigrate into the PCFG in 2000 and 2001.

Although the simulation results could be sensitive to other parameters incorporated in the models, a limited evaluation of the effects of increased carrying capacity for the PCFG or a more recent founding time was conducted. These simulations suggested that to obtain the empirical results presented in Lang *et al.* 2011 under a scenario of no annual immigration, the abundance of the PCFG would have to be larger (>500 animals) than currently estimated. Gray whales have been observed feeding off of Kodiak Island, Alaska since at least 1999, with ~350-400 individuals counted during a single day in July 2000 (Moore *et al.* 2007). Approximately 20% of the animals photographically identified in this area between 2002 and 2005 are known to be animals that have also been photographed in the Pacific Northwest from northern California to southeast Alaska (Gosho *et al.* 2011). However, the median "crossing point" calculated from these comparisons suggest that values of K between 2000 (based on F_{ST}) and 3000 (based on the number of haplotypes) animals produce values that are most consistent with the empirical data, indicating that additional explanation may be needed.

The simulations exploring more recent founding times suggest that under a scenario with no annual immigration, the PCFG would have to have been founded after 1950, and more plausibly between the mid-1960s to mid-1970s, to produce simulated results that are consistent with the empirical data. Small numbers of gray whales have been sighted within the seasonal range of the PCFG since at least 1926 (Howell & Huey 1930, Gilmore 1960, Pike and MacAskie 1969, additional references in Rice & Wolman 1971), but photo-identification studies did not start until the 1970s, when the repeated return of individuals to the area was first documented (Hatler & Darling 1974, Darling 1984). Our simulations model an instantaneous colonization of the PCFG, such that for the scenarios modeling colonization in 1960 or later at least 60 whales become part of the PCFG in a given year. This aspect of our simulations is clearly an oversimplification. Given both the limited information available on use of the PCFG seasonal range prior to the 1970s and the limitations of our model, it is difficult to evaluate how the simulation results fit in with past records.

The simulations incorporating a pre-whaling split of the PCFG from the larger ENP population are in progress and are expected to be completed by the 2012 SC meeting. Future work will also include integrating the genetic data representing ENP gray whales in LeDuc *et al.* 2002 and Lang 2010 with the data represented in Lang *et al.* 2011 to ensure that the diversity values utilized here are as representative as possible of the larger ENP population. Simulations will also be performed to explore the effect of incorporating lower MSYR rates for the PCFG into the life history matrices underlying the models.

REFERENCES

Alter, S.A., E. Rynes, and S.R. Palumbi. 2007. DNA evidence for historic population size and past ecosystem impacts of gray whales. Proceedings of the National Academy of Sciences 104(38):15162-15167.

Archer, F. I., K. K. Martien, et al. 2010. "A simulation-based approach to evaluating population structure in non-equilibrial populations." Journal of Cetacean Research and Management 11: 101-113.

Bradford, A. L., D. W. Weller, A. R. Lang, G. Tsidulko, A. M. Burdin, and R. L. Brownell, Jr. In press. Comparing observations of age at first reproduction in western gray whales to estimates of age at sexual maturity in eastern gray whales. Journal of Cetacean Research and Management.

Calambokidis, J., J.L. Laake and A. Klimek. 2010. Abundance and population structure of seasonal gray whales in the Pacific Northwest, 1998 - 2008. Paper IWC/62/BRG32 submitted to the International Whaling Commission Scientific Committee. 50 pp.

Darling, J.D. 1984. Gray whales (*Eschrichtius robustus*) off Vancouver Island, British Columbia. *in* M.L. Jones, S.L. Swartz and S. Leatherwood, eds. The Gray Whale. Academic Press, Inc., Orlando, FL.

Excoffier, L. and M. Foll. 2011. Fastsimcoal: a continuous-time coalescent simulator of genomic diversity under arbitrarily complex evolutionary scenarios. Bioinformatics.

Gilmore, R. M 1960. A census of the California gray whale. U.S. Fish and Wildlife Service, Special Scientific Reports Fisheries 342:1-30.

Gosho, M., Gearin, P., Jenkinson, R., Laake, J., Mazzuca, L., Kubiak, D., Calambokidis, J., Megill, W., Gisborne B., Goley, D., Tombach, C., Darling, J. and V. Deeke. 2011. Movements and diet of gray whales (*Eschrichtius robustus*) off Kodiak Island, Alaska, 2002-2005. Paper SC/M11/AWMP2 presented to the International Whaling Commission Scientific Committee.

Hatler, D. F. and J. D. Darling. 1974. Recent observations of the gray whale in British Columbia. Canadian Field Naturalist 88: 449-459.

Howell, A. B. and Huey, L. M. 1930. Food of the gray whale and other whales. Journal of Mammalogy 11:321-322.

International Whaling Commission. 2011. Report of the 2011 AWMP workshop with a focus on eastern gray whales. Report SC/63/Rep.2 presented to the International Whaling Commission Scientific Committee. [Available at http;//www.iwcoffice.org]

Lang, A.R. 2010. The population genetics of gray whales (*Eschrichtius robustus*) in the North Pacific. Ph.D. dissertation, University of California San Diego, 222 pp.

Lang, A.R., Taylor, B.L., Calambokidis, J., Pease, V.L., Klimik, A., Scordino, J., Robertson, K.M., Litovka, D., Burkanov, V., Gearin, P., George, J.C. and Mate, B. 2011b. Assessment of stock structure among gray whales utilizing feeding grounds in the Eastern North Pacific. Paper SC/M11/AWMP4 presented to the International Whaling Commission Scientific Committee.

Laval, G. and L. Excoffier. 2004. SIMCOAL 2.0: a program to simulate genomic diversity over large recombining regions in a subdivided population with a complex history. Bioinformatics. 20:2485-2487.

LeDuc, R.G., Weller, D.W., Hyde, J., Burdin, A.M., Rosel, P.E., Brownell, R.L., Würsig, B. and Dizon, A.E. 2002. Genetic differences between western and eastern gray whales (*Eschrichtius robustus*). Journal of Cetacean Research and Management 4:1-5.

Martien, K. K., D. Tallmon, et al. 2008. Life history matrices for TOSSM model. Presented to the International Whaling Commission Scientific Committee: SC/56/SD55.

Martien, K. K. 2006. Progress on TOSSM dataset generation. Presented to the International Whaling Commission Scientific Committee: SC/58/SD52.

Martien, K.K., E.A. Archer, B.J. Ripley, and B.L. Taylor. 2007. The genetic consequences of non-equilibrial dynamics in bowhead whales. Presented to the International Whaling Commission Scientific Committee: SC/59/BRG16.

Martien, K. K., D. Gregovich, et al. 2009. tossm: an R package for assessing performance of genetic analytical methods in a management context. Molecular Ecology Resources 9(6): 1456-1459.

Moore, S.E., K.M. Wynne, J.C. Kinney, and J.M. Grebmeier. 2007. Gray whale occurrence and forage southeast of Kodiak Island, Alaska. Marine Mammal Science 23:419-428.

Pike, G. C. and MacAskie, I. B. 1969. Marine mammals of British Columbia. Bulletin of the Fisheries Research Board of Canada 171:1-54.

Punt, A. E., and P. R. Wade. 2010. Population status of the eastern North Pacific stock of gray whales in 2009. U.S. Dep. Commer. NOAA Tech. Memo. NMFS-AFSC.

Rice, R. W. and Wolman, A. A. 1971. The life history and ecology of the gray whale (*Eschrichtius robustus*). The American Society of Mammalogists, Special issue.

Strand A, 2002. METASIM 1.0: an individual-based environment for simulating population genetics of complex population dynamics. Molecular Ecology Notes 2:373-376.

Table 1. The proportion of birth events in the simulated data that resulted in multiple offspring for the same female in a given year.

	5-stage TOSSM matrices	9-stage matrices
Proportion of single offspring births:	64%	92%
Proportion of multiple offspring births:	36%	8%
Range of multiple offspring births:	2-7	2-3

Table 2. Calving intervals in the simulated datasets.

Measure	5-stage TOSSM matrices	9-stage matrices
Median	3	2
Mean	5.1	3.2
Variance	27.08	16.50
stdev	5.20	4.06
Min	2	1
Max	35	38

Table 3. Vital rates for gray whales. Generation time shown here is calculated based on a maximum age of 40 years (as in previous work).

Vital Rate	5-stage TOSSM matrices		9-stage matrices	
	At K	Near ZPD	At K	Near ZPD
Juvenile survival	0.925	0.94	0.905	0.935
Adult female survival	0.946	0.946	0.982	0.982
Adult male survival	0.954	0.954	0.982	0.982
Calf survival	0.925	0.94	0.732	0.732
Age of first reproduction	10	5	10	7
Rate of increase (λ)	1.003	1.072	1.000	1.064
Generation Time*	19.5	16.9	21.10	20.60

Table 4. The updated stage-based matrices for use at a) zero population density and b) carrying capacity are shown below.

a) Nine-stage matrices at ZPD:

	juv1	juv2	juv3	F1	F2	F3	M1	M2	M3
juv1	0.497	0.000	0.000	0.366	0.366	0.366	0.000	0.000	0.000
juv2	0.438	0.497	0.000	0.000	0.000	0.000	0.000	0.000	0.000
juv3	0.000	0.438	0.497	0.000	0.000	0.000	0.000	0.000	0.000
F1	0.000	0.000	0.219	0.942	0.000	0.000	0.000	0.000	0.000
F2	0.000	0.000	0.000	0.040	0.942	0.000	0.000	0.000	0.000
F3	0.000	0.000	0.000	0.000	0.040	0.942	0.000	0.000	0.000
M1	0.000	0.000	0.219	0.000	0.000	0.040	0.942	0.000	0.000
M2	0.000	0.000	0.000	0.000	0.000	0.000	0.040	0.942	0.000
M3	0.000	0.000	0.000	0.000	0.000	0.000	0.000	0.040	0.942

b) Nine-stage matrices at K:

	juv1	juv2	juv3	F1	F2	F3	M1	M2	M3
juv1	0.633	0.000	0.000	0.176	0.176	0.176	0.000	0.000	0.000
juv2	0.272	0.633	0.000	0.000	0.000	0.000	0.000	0.000	0.000
juv3	0.000	0.272	0.633	0.000	0.000	0.000	0.000	0.000	0.000
F1	0.000	0.000	0.136	0.914	0.000	0.000	0.000	0.000	0.000
F2	0.000	0.000	0.000	0.068	0.914	0.000	0.000	0.000	0.000
F3	0.000	0.000	0.000	0.000	0.068	0.914	0.000	0.000	0.000
M1	0.000	0.000	0.136	0.000	0.000	0.068	0.914	0.000	0.000
M2	0.000	0.000	0.000	0.000	0.000	0.000	0.068	0.914	0.000
M3	0.000	0.000	0.000	0.000	0.000	0.000	0.000	0.068	0.914

c) Five-stage(TOSSM) matrices at ZPD:

	juv1	juv2	fert	lact	male
juv1	0.730	0.000	0.000	0.940	0.000
juv2	0.210	0.000	0.000	0.000	0.000
fert	0.000	0.470	0.000	0.946	0.000
lact	0.000	0.000	0.946	0.000	0.000
male	0.000	0.470	0.000	0.000	0.954

d) Five-stage (TOSSM) matrices at K:

	juv1	juv2	fert	lact	male
juv1	0.768	0.000	0.000	0.925	0.000
juv2	0.157	0.720	0.000	0.000	0.000
fert	0.000	0.102	0.648	0.946	0.000
lact	0.000	0.000	0.298	0.000	0.000
male	0.000	0.102	0.000	0.000	0.954

Figure 5. Examples of trajectories for PCFG, under a model incorporating a post-whaling split with pulse immigration. Plots for the abundance of the PCFG whales span 1930 to 2010, while the plot showing the abundance of the larger ENP population spans 1846 to 2010 to show the simulated depletion due to commercial whaling.
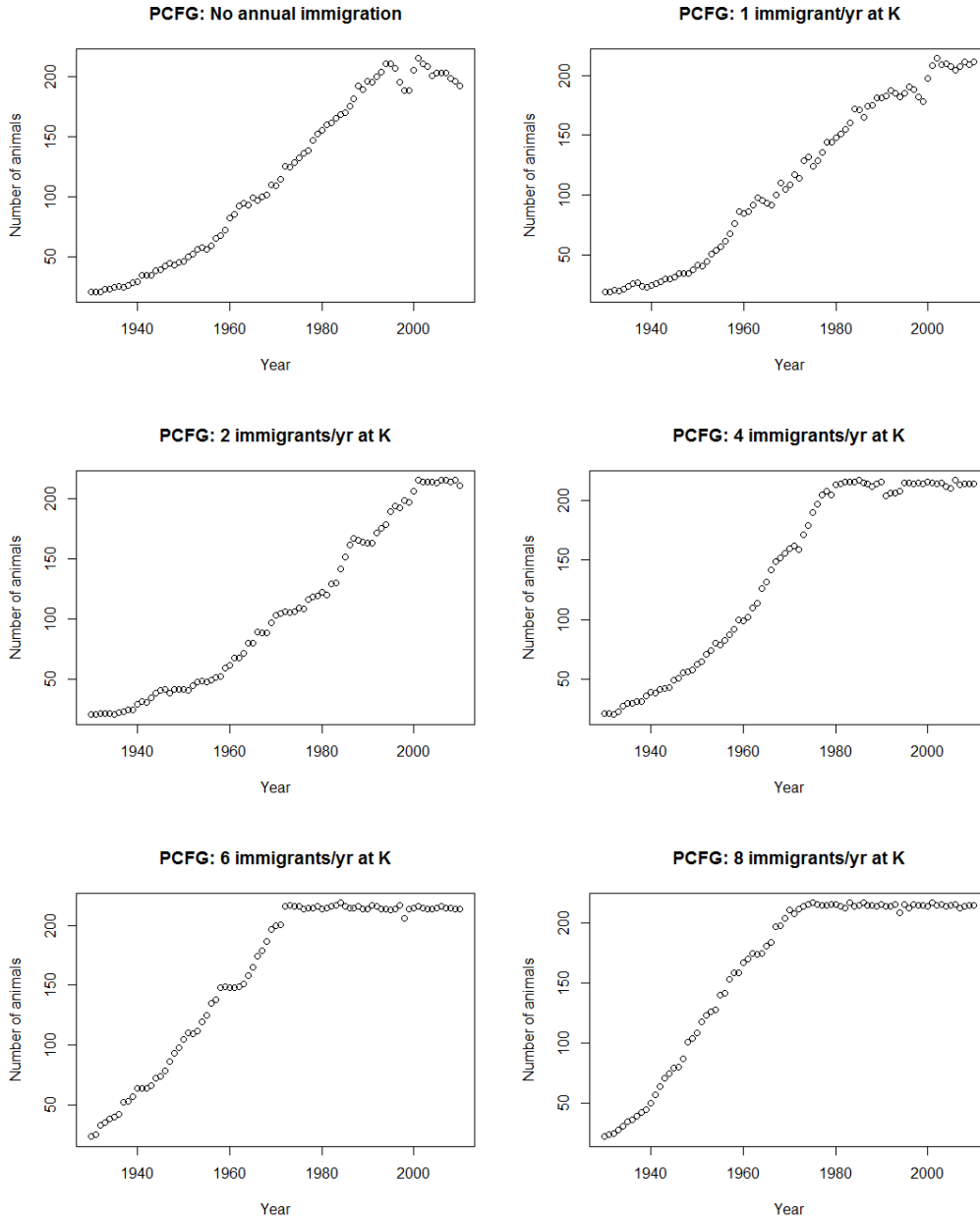
PCFG: 10 immigrants/yr at K
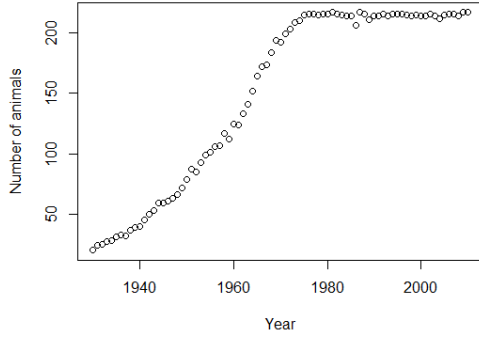
PCFG: 12 immigrants/yr at K
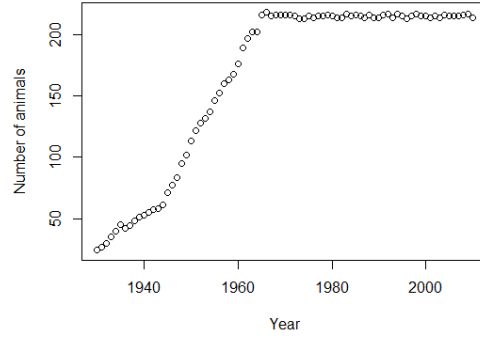
PCFG: 14 immigrants/yr at K
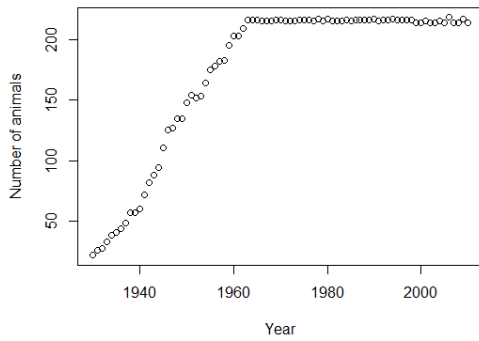
PCFG: 16 immigrants/yr at K
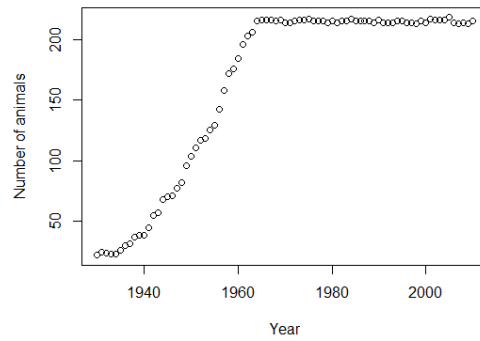
ENP

Figure 6. Example of the number of immigrants per year generated for one replicate (9-stage matrices with pulse immigration). The dotted line represents the number of immigrants per year that would be expected when the ENP population reaches K.

Annual immigration at K = 12

Annual immigration at K = 14

Annual immigration at K = 16

Table 7. List of scenarios that have been completed for 100 replications.

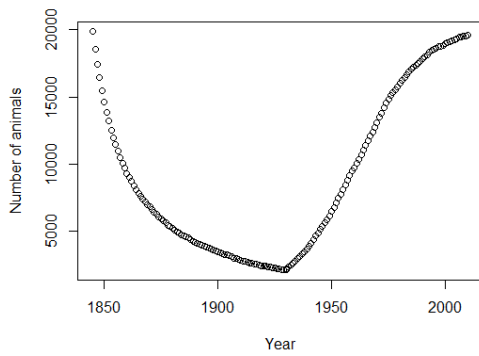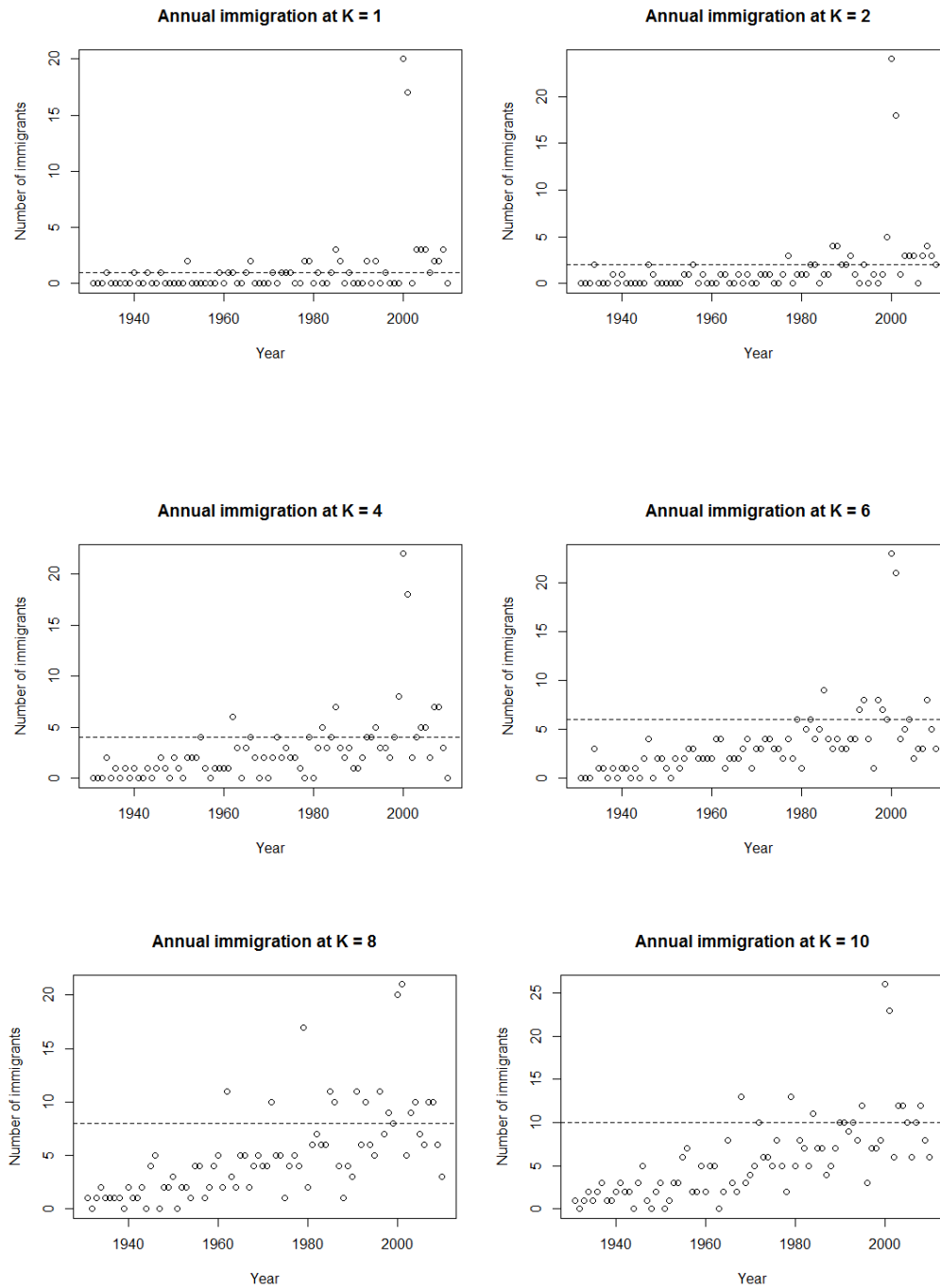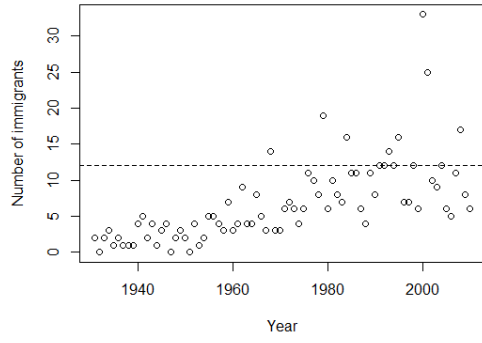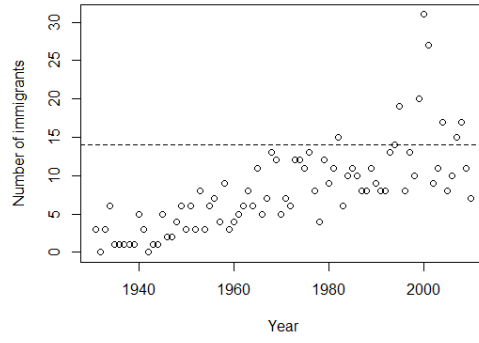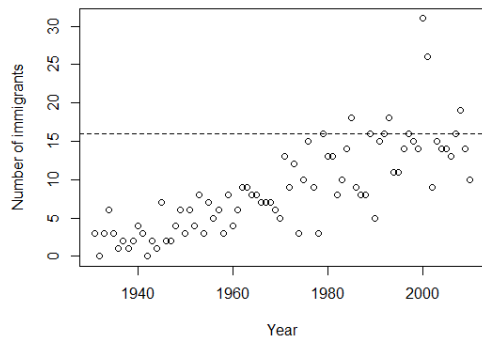| Index	Matrices	Timing of split	Year of split	PCFG Carrying Capacity (K)	Immigrants/yr into the PCFG (at K)	Pulse immigration
1	9-stage	Post-whaling split	1930	200	0	Y
2	9-stage	Post-whaling split	1930	200	1	Y
3	9-stage	Post-whaling split	1930	200	2	Y
4	9-stage	Post-whaling split	1930	200	4	Y
5	9-stage	Post-whaling split	1930	200	6	Y
6	9-stage	Post-whaling split	1930	200	8	Y
7	9-stage	Post-whaling split	1930	200	10	Y
8	9-stage	Post-whaling split	1930	200	12	Y
9	9-stage	Post-whaling split	1930	200	14	Y
10	9-stage	Post-whaling split	1930	200	16	Y
11	9-stage	Post-whaling split	1930	200	0	N
12	9-stage	Post-whaling split	1930	200	1	N
13	9-stage	Post-whaling split	1930	200	2	N
14	9-stage	Post-whaling split	1930	200	4	N
15	9-stage	Post-whaling split	1930	200	6	N
16	9-stage	Post-whaling split	1930	200	8	N
17	9-stage	Post-whaling split	1930	200	10	N
18	9-stage	Post-whaling split	1930	200	12	N
19	9-stage	Post-whaling split	1930	200	14	N
20	9-stage	Post-whaling split	1930	200	16	N
21	5-stage	Post-whaling split	1930	200	0	Y
22	5-stage	Post-whaling split	1930	200	1	Y
23	5-stage	Post-whaling split	1930	200	2	Y
24	5-stage	Post-whaling split	1930	200	4	Y
25	5-stage	Post-whaling split	1930	200	6	Y
26	5-stage	Post-whaling split	1930	200	8	Y
27	5-stage	Post-whaling split	1930	200	10	Y
28	5-stage	Post-whaling split	1930	200	12	Y
29	5-stage	Post-whaling split	1930	200	14	Y
30	5-stage	Post-whaling split	1930	200	16	Y
31	9-stage	Post-whaling split	1940	200	0	Y
32	9-stage	Post-whaling split	1950	200	0	Y
33	9-stage	Post-whaling split	1960	200	0	Y
34	9-stage	Post-whaling split	1970	200	0	Y
35	9-stage	Post-whaling split	1980	200	0	Y
36	9-stage	Post-whaling split	1990	200	0	Y
37	9-stage	Post-whaling split	1930	500	0	Y
38	9-stage	Post-whaling split	1930	1000	0	Y
39	9-stage	Post-whaling split	1930	1500	0	Y
40	9-stage	Post-whaling split	1930	2000	0	Y
41	9-stage	Post-whaling split	1930	3000	0	Y
42	9-stage	Post-whaling split	1930	5000	0	Y

* Pulse immigration consists of +20 animals in per year as reflected in the abundance in 2000 and 2001

Table 8. The number of samples collected per year from each stratum in the Lang *et al.* 2011 study.

Year	North	PCFG
1994	11	0
1995	0	0
1996	0	3
1997	1	3
1998	0	7
1999	1	0
2000	1	2
2001	27	0
2002	0	1
2003	12	3
2004	12	3
2005	10	1
2006	0	0
2007	0	0
2008	0	0
2009	0	13
2010	28	35
Total	103	71

Table 9. Summary of the haplotypic diversity, number of mtDNA haplotypes, and nucleotide diversity generated in the simulated ENP population. Only the results from the post-whaling split with immigration pulse models are shown as results were similar under all other models.

Haplotypic diversity:

ENP: H_{obs} =0.952

Matrices	Scenario	Immigration (Inds/Yr at K)	With pulse?	Median_ENP	Min_ENP	Max_ENP	Prop < than ENP	Prop > than ENP
9-stage	Post-whaling split	0	Y	0.948	0.883	0.973	61	39
9-stage	Post-whaling split	1	Y	0.951	0.869	0.973	52	48
9-stage	Post-whaling split	2	Y	0.950	0.878	0.974	56	44
9-stage	Post-whaling split	4	Y	0.950	0.874	0.974	57	43
9-stage	Post-whaling split	6	Y	0.950	0.890	0.972	56	44
9-stage	Post-whaling split	8	Y	0.948	0.869	0.973	64	36
9-stage	Post-whaling split	10	Y	0.949	0.878	0.977	62	38
9-stage	Post-whaling split	12	Y	0.950	0.786	0.971	54	46
9-stage	Post-whaling split	14	Y	0.948	0.862	0.973	61	39
9-stage	Post-whaling split	16	Y	0.950	0.877	0.977	52	48

Number of haplotypes:

ENP: Nb_haps_{obs}=32

Matrices	Scenario	Immigration (Inds/Yr at K)	With pulse?	Median_ENP	Min_ENP	Max_ENP	Prop < than ENP	Prop > than ENP
9-stage	Post-whaling split	0	Y	33	25	47	36	52
9-stage	Post-whaling split	1	Y	33	24	44	33	57
9-stage	Post-whaling split	2	Y	33	23	46	40	54
9-stage	Post-whaling split	4	Y	33	22	44	37	54
9-stage	Post-whaling split	6	Y	34	24	42	25	62
9-stage	Post-whaling split	8	Y	33	22	45	38	55
9-stage	Post-whaling split	10	Y	33	20	45	38	54
9-stage	Post-whaling split	12	Y	33	20	43	37	57
9-stage	Post-whaling split	14	Y	33	23	44	38	52
9-stage	Post-whaling split	16	Y	33	25	45	31	56

Nucleotide diversity:

ENP: $\prod_{obs}$ = 0.0142

Matrices	Scenario	Immigration (Inds/Yr at K)	With pulse?	Median_ENP	Min_ENP	Max_ENP	Prop < than ENP	Prop > than ENP
9-stage	Post-whaling split	0	Y	0.026	0.012	0.065	7	93
9-stage	Post-whaling split	1	Y	0.025	0.011	0.060	10	90
9-stage	Post-whaling split	2	Y	0.024	0.012	0.056	9	91
9-stage	Post-whaling split	4	Y	0.025	0.011	0.059	9	91
9-stage	Post-whaling split	6	Y	0.025	0.011	0.060	10	90
9-stage	Post-whaling split	8	Y	0.025	0.011	0.067	8	92
9-stage	Post-whaling split	10	Y	0.024	0.011	0.059	8	92
9-stage	Post-whaling split	12	Y	0.025	0.010	0.057	9	91
9-stage	Post-whaling split	14	Y	0.025	0.011	0.071	7	93
9-stage	Post-whaling split	16	Y	0.025	0.011	0.066	9	91

Figure 10. Histogram showing the distribution of p-values for a χ² test comparing the observed to the simulated haplotype distributions for the larger ENP population.
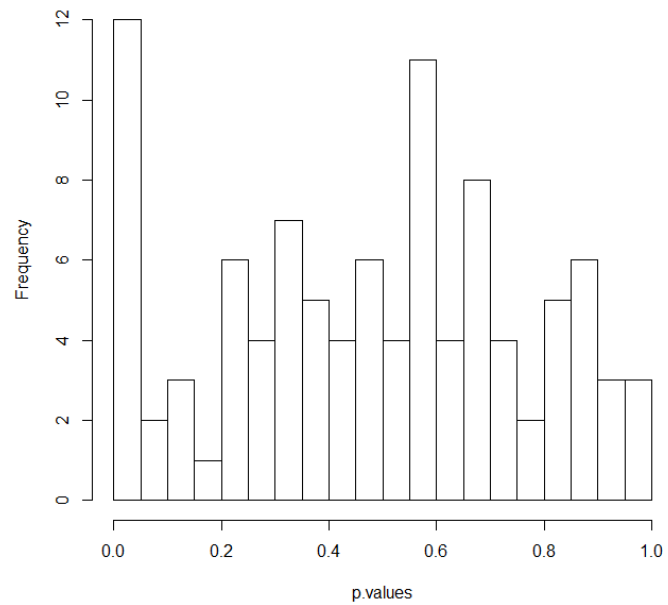
Figure 11. Graphical representation of the proportion of simulated values that are lower (shown in black) or higher (shown in gray) than the observed value generated from the empirical data. Simulated values are derived from the model incorporating a post-whaling split with pulse migration under the nine-stage matrices.
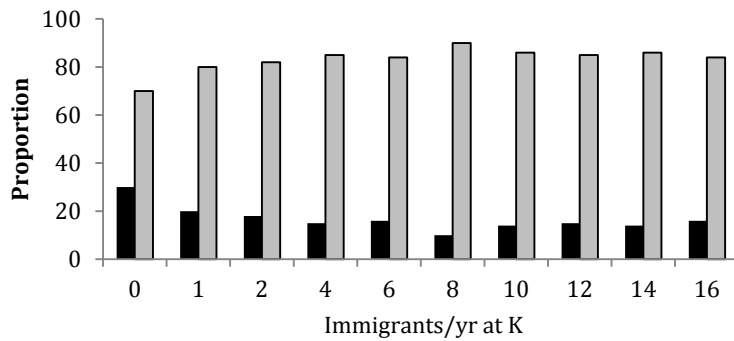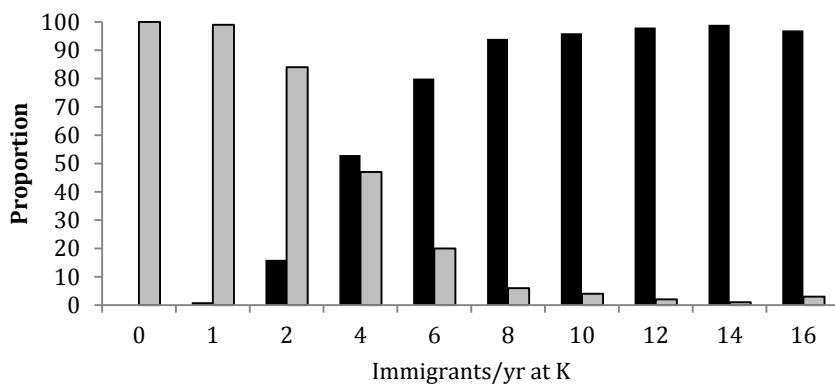
a.) Number of haplotypes:
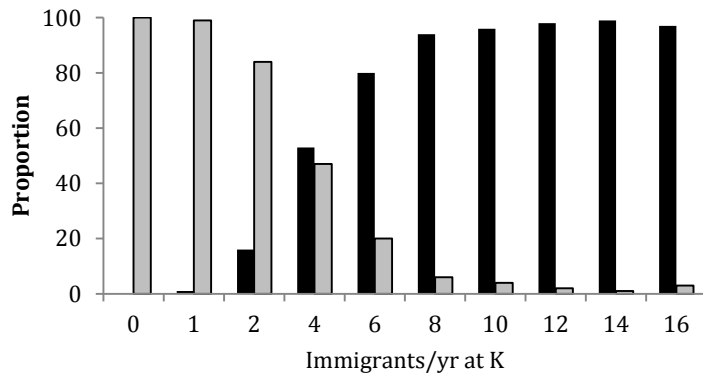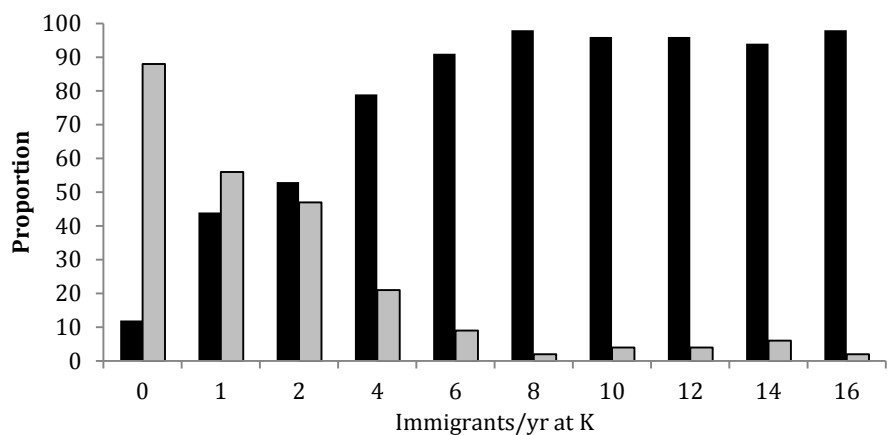

b.) Haplotypic diversity:
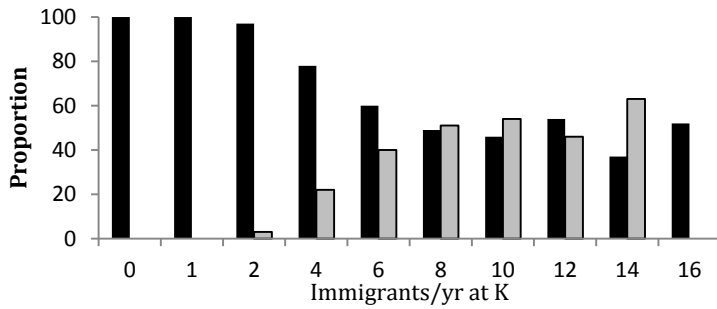
c.) Nucleotide diversity:

d.) F_{ST}:

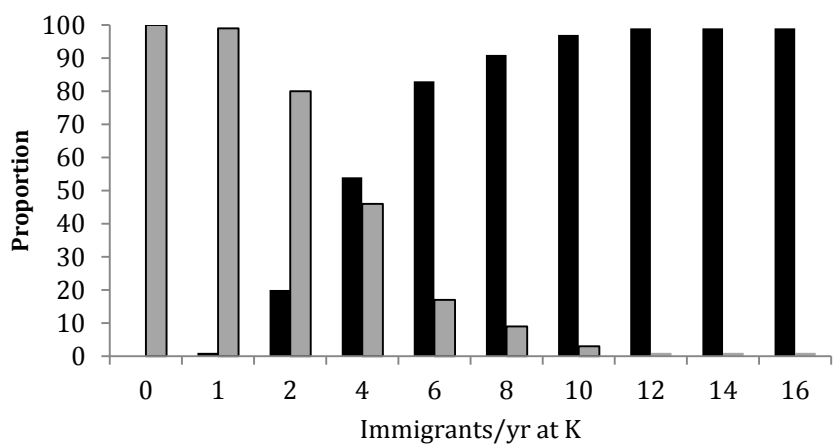e.) ϕ_{ST}:

f.) χ^2/df:

Table 12. Summary of number of mtDNA haplotypes in the simulated data for the PCFG. Scenarios highlighted in bold type produced results which were not consistent with those based on the empirical data.

PCFG: Nb_haps $_{obs}$=23

Matrices	Scenario	Immigrants/yr (at K)	With pulse?	Median_PCFG	Min_PCFG	Max_PCFG	Prop < PCFG	Prop > than obs
9-stage	**Post-whaling split**	**0**	**Y**	**12.0**	**6**	**19**	**100**	**0**
9-stage	**Post-whaling split**	**1**	**Y**	**16.6**	**11**	**26**	**96**	**2**
9-stage	Post-whaling split	2	Y	19.8	11	30	78	12
9-stage	Post-whaling split	4	Y	23.1	14	32	41	48
9-stage	Post-whaling split	6	Y	25.0	14	36	22	71
9-stage	Post-whaling split	8	Y	25.7	16	33	15	75
9-stage	Post-whaling split	10	Y	27.2	18	35	9	84
9-stage	Post-whaling split	12	Y	26.3	16	34	14	80
9-stage	Post-whaling split	14	Y	27.5	21	36	10	83
9-stage	Post-whaling split	16	Y	27.1	16	38	11	83
9-stage	**Post-whaling split**	**0**	**N**	**6.4**	**3**	**12**	**100**	**0**
9-stage	**Post-whaling split**	**1**	**N**	**12.5**	**6**	**20**	**100**	**0**
9-stage	**Post-whaling split**	**2**	**N**	**17.1**	**8**	**24**	**97**	**1**
9-stage	Post-whaling split	4	N	22.5	15	40	49	38
9-stage	Post-whaling split	6	N	23.9	12	32	36	52
9-stage	Post-whaling split	8	N	25.4	14	38	22	73
9-stage	Post-whaling split	10	N	25.8	17	37	27	66
9-stage	Post-whaling split	12	N	26.6	17	33	11	86
9-stage	Post-whaling split	14	N	27.0	17	36	11	84
9-stage	Post-whaling split	16	N	26.7	18	38	16	76
5-stage	**Post-whaling split**	**0**	**Y**	**10.4**	**6**	**16**	**100**	**0**
5-stage	**Post-whaling split**	**1**	**Y**	**15.0**	**7**	**23**	**99**	**0**
5-stage	Post-whaling split	2	Y	18.1	9	26	88	8
5-stage	Post-whaling split	4	Y	21.5	15	30	60	29
5-stage	Post-whaling split	6	Y	22.9	15	30	49	38
5-stage	Post-whaling split	8	Y	24.1	18	35	33	56
5-stage	Post-whaling split	10	Y	24.6	17	37	29	61
5-stage	Post-whaling split	12	Y	25.0	17	35	28	65
5-stage	Post-whaling split	14	Y	24.8	18	34	30	63
5-stage	Post-whaling split	16	Y	25.4	17	37	21	67

Table 13. Summary of haplotypic diversity in the simulated data for the PCFG. Scenarios highlighted in bold type produced results which were not consistent with those based on the empirical data.

PCFG: Hobs = 0.945

Matrices	Scenario	Immigration (Inds/Yr at K)	With pulse?	Median_PCFG	Min_PCFG	Max_PCFG	Prop < than PCFG	Prop > than PCFG
9-stage	**Post-whaling split**	**0**	**Y**	**0.804**	**0.137**	**0.896**	**100**	**0**
9-stage	**Post-whaling split**	**1**	**Y**	**0.869**	**0.334**	**0.940**	**100**	**0**
9-stage	**Post-whaling split**	**2**	**Y**	**0.907**	**0.722**	**0.949**	**97**	**3**
9-stage	Post-whaling split	4	Y	0.933	0.699	0.970	78	22
9-stage	Post-whaling split	6	Y	0.939	0.810	0.971	60	40
9-stage	Post-whaling split	8	Y	0.945	0.848	0.972	49	51
9-stage	Post-whaling split	10	Y	0.948	0.857	0.974	46	54
9-stage	Post-whaling split	12	Y	0.943	0.825	0.969	54	46
9-stage	Post-whaling split	14	Y	0.951	0.842	0.972	37	63
9-stage	Post-whaling split	16	Y	0.944	0.866	0.979	52	48
9-stage	**Post-whaling split**	**0**	**N**	**0.754**	**0.344**	**0.867**	**100**	**0**
9-stage	**Post-whaling split**	**1**	**N**	**0.841**	**0.608**	**0.928**	**100**	**0**
9-stage	**Post-whaling split**	**2**	**N**	**0.888**	**0.748**	**0.946**	**99**	**1**
9-stage	Post-whaling split	4	N	0.932	0.788	0.974	84	16
9-stage	Post-whaling split	6	N	0.936	0.840	0.965	67	33
9-stage	Post-whaling split	8	N	0.941	0.835	0.974	59	41
9-stage	Post-whaling split	10	N	0.944	0.842	0.977	51	49
9-stage	Post-whaling split	12	N	0.946	0.870	0.971	45	55
9-stage	Post-whaling split	14	N	0.946	0.878	0.976	43	57
9-stage	Post-whaling split	16	N	0.947	0.841	0.976	48	52
5-stage	**Post-whaling split**	**0**	**Y**	**0.734**	**0.259**	**0.883**	**100**	**0**
5-stage	**Post-whaling split**	**1**	**Y**	**0.854**	**0.600**	**0.930**	**100**	**0**
5-stage	**Post-whaling split**	**2**	**Y**	**0.890**	**0.717**	**0.949**	**97**	**3**
5-stage	Post-whaling split	4	Y	0.915	0.752	0.958	92	8
5-stage	Post-whaling split	6	Y	0.929	0.768	0.963	79	21
5-stage	Post-whaling split	8	Y	0.931	0.796	0.965	74	26
5-stage	Post-whaling split	10	Y	0.934	0.720	0.973	78	22
5-stage	Post-whaling split	12	Y	0.935	0.747	0.968	64	36
5-stage	Post-whaling split	14	Y	0.937	0.823	0.965	67	33
5-stage	Post-whaling split	16	Y	0.934	0.834	0.971	68	32

Table 14. Summary of the mtDNA nucleotide diversity in the simulated data for the PCFG. Scenarios highlighted in bold type produced results which were not consistent with those based on the empirical data.

PCFG: $\prod$ obs = 0.0148

Matrices	Scenario	Immigration (Inds/Yr at K)	With pulse?	Median_PCFG	Min_PCFG	Max_PCFG	Prop < than PCFG	Prop > than PCFG
9-stage	Post-whaling split	0	Y	0.021	0.004	0.059	30	70
9-stage	Post-whaling split	1	Y	0.022	0.005	0.056	20	80
9-stage	Post-whaling split	2	Y	0.022	0.010	0.063	18	82
9-stage	Post-whaling split	4	Y	0.025	0.010	0.062	15	85
9-stage	Post-whaling split	6	Y	0.025	0.010	0.062	16	84
9-stage	Post-whaling split	8	Y	0.025	0.012	0.066	10	90
9-stage	Post-whaling split	10	Y	0.025	0.010	0.058	14	86
9-stage	Post-whaling split	12	Y	0.025	0.011	0.059	15	85
9-stage	Post-whaling split	14	Y	0.025	0.011	0.059	14	86
9-stage	Post-whaling split	16	Y	0.024	0.010	0.067	16	84
9-stage	Post-whaling split	0	N	0.020	0.002	0.080	32	68
9-stage	Post-whaling split	1	N	0.022	0.007	0.051	27	73
9-stage	Post-whaling split	2	N	0.023	0.007	0.064	18	82
9-stage	Post-whaling split	4	N	0.024	0.008	0.062	15	85
9-stage	Post-whaling split	6	N	0.025	0.010	0.064	13	87
9-stage	Post-whaling split	8	N	0.024	0.010	0.060	11	89
9-stage	Post-whaling split	10	N	0.026	0.010	0.074	14	86
9-stage	Post-whaling split	12	N	0.025	0.010	0.065	12	88
9-stage	Post-whaling split	14	N	0.025	0.011	0.059	12	88
9-stage	Post-whaling split	16	N	0.025	0.010	0.058	12	88
5-stage	Post-whaling split	0	Y	0.015	0.004	0.042	51	49
5-stage	Post-whaling split	1	Y	0.018	0.003	0.046	44	56
5-stage	Post-whaling split	2	Y	0.018	0.005	0.048	37	63
5-stage	Post-whaling split	4	Y	0.017	0.005	0.051	27	73
5-stage	Post-whaling split	6	Y	0.019	0.005	0.054	27	73
5-stage	Post-whaling split	8	Y	0.020	0.006	0.048	31	69
5-stage	Post-whaling split	10	Y	0.020	0.004	0.053	31	69
5-stage	Post-whaling split	12	Y	0.020	0.005	0.052	27	73
5-stage	Post-whaling split	14	Y	0.021	0.005	0.052	29	71
5-stage	Post-whaling split	16	Y	0.020	0.006	0.050	25	75

Table 15. Summary of F_{ST} values generated in the comparison of simulated data representing the PCFG and the larger ENP population. Scenarios highlighted in bold type produced results which were not consistent with those based on the empirical data.

$F_{ST\ obs} = 0.012$

Matrices	Scenario	Immigration (Inds/Yr at K)	With pulse?	Median	Min	Max	Prop > than obseved	Prop > than observed
9-stage	**post-whaling split**	**0**	**Y**	**0.069**	**0.019**	**0.254**	**0**	**100**
9-stage	**post-whaling split**	**1**	**Y**	**0.040**	**0.005**	**0.189**	**1**	**99**
9-stage	post-whaling split	2	Y	0.023	0.002	0.096	16	84
9-stage	post-whaling split	4	Y	0.011	-0.004	0.033	53	47
9-stage	post-whaling split	6	Y	0.005	-0.005	0.030	80	20
9-stage	post-whaling split	8	Y	0.002	-0.004	0.017	94	6
9-stage	**post-whaling split**	**10**	**Y**	**0.002**	**-0.007**	**0.021**	**96**	**4**
9-stage	**post-whaling split**	**12**	**Y**	**0.001**	**-0.006**	**0.019**	**98**	**2**
9-stage	**post-whaling split**	**14**	**Y**	**0.001**	**-0.007**	**0.013**	**99**	**1**
9-stage	**post-whaling split**	**16**	**Y**	**0.001**	**-0.007**	**0.020**	**97**	**3**
9-stage	**post-whaling split**	**0**	**N**	**0.099**	**0.029**	**0.295**	**0**	**100**
9-stage	**post-whaling split**	**1**	**N**	**0.051**	**0.020**	**0.146**	**0**	**100**
9-stage	post-whaling split	2	N	0.032	0.006	0.098	9	91
9-stage	post-whaling split	4	N	0.012	-0.004	0.058	47	53
9-stage	post-whaling split	6	N	0.008	-0.003	0.035	71	29
9-stage	post-whaling split	8	N	0.003	-0.004	0.025	91	9
9-stage	post-whaling split	10	N	0.003	-0.006	0.022	93	7
9-stage	**post-whaling split**	**12**	**N**	**0.001**	**-0.007**	**0.015**	**98**	**2**
9-stage	**post-whaling split**	**14**	**N**	**0.002**	**-0.007**	**0.016**	**98**	**2**
9-stage	**post-whaling split**	**16**	**N**	**0.001**	**-0.006**	**0.048**	**92**	**8**
5-stage	**post-whaling split**	**0**	**Y**	**0.101**	**0.018**	**0.323**	**0**	**100**
5-stage	post-whaling split	1	Y	0.044	0.007	0.150	6	94
5-stage	post-whaling split	2	Y	0.025	-0.002	0.097	18	82
5-stage	post-whaling split	4	Y	0.009	-0.004	0.045	64	36
5-stage	post-whaling split	6	Y	0.004	-0.008	0.040	87	13
5-stage	post-whaling split	8	Y	0.002	-0.004	0.021	90	10
5-stage	post-whaling split	10	Y	0.003	-0.005	0.025	94	6
5-stage	**post-whaling split**	**12**	**Y**	**0.001**	**-0.007**	**0.014**	**96**	**4**
5-stage	**post-whaling split**	**14**	**Y**	**0.001**	**-0.006**	**0.016**	**98**	**2**
5-stage	**post-whaling split**	**16**	**Y**	**0.000**	**-0.006**	**0.019**	**97**	**3**

Table 16. Summary of ϕ_{ST} values generated in the comparison of simulated data representing the PCFG and the larger ENP population. Scenarios highlighted in bold type produced results which were not consistent with those based on the empirical data.

$\phi_{STobs}=0.023$

Matrices	Scenario	Immigration (Inds/Yr at K)	With pulse?	Median	Min	Max	Prop > than observed	Prop < than observed
9-stage	Arch1_sc1	0	Y	0.065	0.000	0.332	12	88
9-stage	Arch1_sc2	1	Y	0.030	-0.002	0.240	44	56
9-stage	Arch1_sc3	2	Y	0.021	-0.004	0.080	53	47
9-stage	Arch1_sc4	4	Y	0.007	-0.009	0.074	79	21
9-stage	Arch1_sc5	6	Y	0.000	-0.011	0.062	91	9
9-stage	**Arch1_sc6**	**8**	**Y**	**-0.001**	**-0.011**	**0.036**	**98**	**2**
9-stage	**Arch1_sc7**	**10**	**Y**	**0.000**	**-0.011**	**0.028**	**96**	**4**
9-stage	**Arch1_sc8**	**12**	**Y**	**-0.003**	**-0.011**	**0.055**	**96**	**4**
9-stage	Arch1_sc9	14	Y	0.000	-0.011	0.044	94	6
9-stage	**Arch1_sc9**	**16**	**Y**	**-0.001**	**-0.010**	**0.032**	**98**	**2**
9-stage	Arch1_sc1	0	N	0.090	0.005	0.439	7	93
9-stage	Arch1_sc2	1	N	0.043	0.002	0.237	23	77
9-stage	Arch1_sc3	2	N	0.026	-0.008	0.187	48	52
9-stage	Arch1_sc4	4	N	0.009	-0.010	0.064	84	16
9-stage	Arch1_sc5	6	N	0.007	-0.009	0.087	86	14
9-stage	Arch1_sc6	8	N	0.001	-0.011	0.071	87	13
9-stage	Arch1_sc7	10	N	-0.002	-0.011	0.051	93	7
9-stage	Arch1_sc8	12	N	-0.002	-0.011	0.037	93	7
9-stage	Arch1_sc9	14	N	-0.001	-0.010	0.040	93	7
9-stage	Arch1_sc10	16	N	-0.002	-0.010	0.092	94	6
5-stage	Arch1_sc1	0	Y	0.099	0.007	0.501	7	93
5-stage	Arch1_sc2	1	Y	0.032	-0.004	0.321	40	60
5-stage	Arch1_sc3	2	Y	0.014	-0.008	0.181	67	33
5-stage	Arch1_sc4	4	Y	0.005	-0.007	0.068	83	17
5-stage	Arch1_sc5	6	Y	0.002	-0.010	0.044	95	5
5-stage	Arch1_sc6	8	Y	0.000	-0.010	0.108	88	12
5-stage	**Arch1_sc7**	**10**	**Y**	**0.001**	**-0.010**	**0.051**	**95**	**5**
5-stage	**Arch1_sc8**	**12**	**Y**	**-0.003**	**-0.011**	**0.045**	**99**	**1**
5-stage	Arch1_sc9	14	Y	-0.002	-0.010	0.044	94	6
5-stage	Arch1_sc9	16	Y	-0.002	-0.011	0.042	94	6

Table 17. Summary of χ^2/df values generated in the comparison of simulated data representing the PCFG and the larger ENP population. Scenarios highlighted in bold type produced results which were not consistent with those based on the empirical data.

χ^2/df $_{obs}$ = 1.42

Matrices	Scenario	Immigration (Inds/Yr at K)	With pulse?	Median	Min	Max	Prop.< than observed	Prop.> than observed
9-stage	**Arch1_sc1**	**0**	**Y**	**2.65**	**1.57**	**3.66**	**0**	**100**
9-stage	**Arch1_sc2**	**1**	**Y**	**2.05**	**1.41**	**3.49**	**1**	**99**
9-stage	Arch1_sc3	2	Y	1.70	1.00	2.87	20	80
9-stage	Arch1_sc4	4	Y	1.41	0.85	2.13	54	46
9-stage	Arch1_sc5	6	Y	1.19	0.74	1.71	83	17
9-stage	Arch1_sc6	8	Y	1.11	0.77	1.69	91	9
9-stage	**Arch1_sc7**	**10**	**Y**	**1.07**	**0.66**	**1.51**	**97**	**3**
9-stage	**Arch1_sc8**	**12**	**Y**	**1.05**	**0.63**	**1.53**	**99**	**1**
9-stage	**Arch1_sc9**	**14**	**Y**	**1.06**	**0.59**	**1.43**	**99**	**1**
9-stage	**Arch1_sc9**	**16**	**Y**	**1.03**	**0.74**	**1.55**	**99**	**1**
9-stage	**Arch1_sc1**	**0**	**N**	**3.23**	**1.87**	**4.73**	**0**	**100**
9-stage	**Arch1_sc2**	**1**	**N**	**2.38**	**1.52**	**3.74**	**0**	**100**
9-stage	Arch1_sc3	2	N	1.93	1.25	3.21	9	91
9-stage	Arch1_sc4	4	N	1.47	0.94	2.12	43	57
9-stage	Arch1_sc5	6	N	1.30	0.81	2.02	73	27
9-stage	Arch1_sc6	8	N	1.16	0.71	1.76	84	16
9-stage	Arch1_sc7	10	N	1.14	0.71	1.62	91	9
9-stage	**Arch1_sc8**	**12**	**N**	**1.07**	**0.70**	**1.80**	**95**	**5**
9-stage	**Arch1_sc9**	**14**	**N**	**1.08**	**0.76**	**1.58**	**96**	**4**
9-stage	**Arch1_sc10**	**16**	**N**	**1.04**	**0.71**	**1.77**	**95**	**5**
5-stage	**Arch1_sc1**	**0**	**Y**	**2.87**	**1.50**	**4.41**	**0**	**100**
5-stage	**Arch1_sc2**	**1**	**Y**	**2.16**	**1.07**	**3.90**	**5**	**95**
5-stage	Arch1_sc3	2	Y	1.71	0.92	2.62	18	82
5-stage	Arch1_sc4	4	Y	1.32	0.82	1.89	64	36
5-stage	Arch1_sc5	6	Y	1.20	0.55	1.64	93	7
5-stage	Arch1_sc6	8	Y	1.12	0.68	1.67	94	6
5-stage	Arch1_sc7	10	Y	1.12	0.71	1.67	92	8
5-stage	**Arch1_sc8**	**12**	**Y**	**1.04**	**0.69**	**1.59**	**97**	**3**
5-stage	**Arch1_sc9**	**14**	**Y**	**1.02**	**0.64**	**1.47**	**98**	**2**
5-stage	**Arch1_sc9**	**16**	**Y**	**1.01**	**0.70**	**1.48**	**99**	**1**

Table 18. Measures of haplotypic diversity, number of haplotypes, and F_{ST} values produced in simulations incorporating a split of the PCFG between 1940 and 1990. These simulations utilized a model incorporating pulse migration and no annual immigration into the PCFG. Scenarios highlighted in bold type produced results which were not consistent with those based on the empirical data.

Haplotypic diversity:
PCFG: H_{obs} = 0.945

Year of split	Median_PCFG	Min_PCFG	Max_PCFG	Prop < than PCFG	Prop > than PCFG
1940	**0.863**	**0.591**	**0.925**	**100**	**0**
1950	**0.884**	**0.721**	**0.932**	**100**	**0**
1960	**0.905**	**0.766**	**0.950**	**98**	**2**
1970	0.927	0.821	0.963	80	20
1980	0.939	0.804	0.969	68	32
1990	0.942	0.883	0.969	55	45

Number of haplotypes
PCFG: Nb_{obs}=23

1940	**14**	**7**	**20**	**100**	**0**
1950	**16**	**10**	**23**	**99**	**0**
1960	**17**	**11**	**23**	**96**	**0**
1970	21.5	12	28	65	22
1980	24	15	33	33	57
1990	25	17	34	25	68

F_{ST}
$F_{ST\ obs}$ = 0.012

1940	**0.046**	**0.008**	**0.177**	**1**	**99**
1950	**0.036**	**0.011**	**0.104**	**1**	**99**
1960	0.022	0.003	0.077	16	84
1970	0.009	-0.005	0.029	64	36
1980	0.006	-0.003	0.035	84	16
1990	**0.003**	**-0.005**	**0.015**	**97**	**3**

Table 19. Measures of haplotypic diversity, number of haplotypes, and F_{ST} values produced in simulations incorporating a carrying capacity for the PCFG ranging from 500 to 5000 animals. These simulations utilized a model incorporating pulse migration and no annual immigration into the PCFG. Scenarios highlighted in bold type produced results which were not consistent with those based on the empirical data.

Haplotypic diversity:
PCFG: H_{obs} = 0.945

K-PCFG	Median_PCFG	Min_PCFG	Max_PCFG	Prop < than PCFG	Prop > than PCFG
500	**0.876**	**0.714**	**0.937**	**100**	**0**
1000	**0.911**	**0.808**	**0.949**	**96**	**4**
1500	0.922	0.818	0.959	90	10
2000	0.932	0.765	0.966	72	28
3000	0.934	0.841	0.965	73	27
5000	0.945	0.849	0.967	47	53

Number of haplotypes
PCFG: Nb_{obs}=23

500	**14**	**7**	**24**	**99**	**1**
1000	**17**	**9**	**23**	**98**	**0**
1500	20	12	27	90	5
2000	20.5	15	28	69	21
3000	22	15	32	51	40
5000	26	16	34	20	73

F_{ST}
F_{ST}obs = 0.012

500	**0.037**	**0.013**	**0.111**	**0**	**100**
1000	0.021	0.006	0.058	21	79
1500	0.015	0.002	0.044	39	61
2000	0.012	-0.002	0.041	52	48
3000	0.007	-0.003	0.025	74	26
5000	0.006	-0.004	0.019	91	9

Table 20. Example trajectories for simulations with K$_{PCFG}$ set between 500 and 5000. Note that scale of y-axis differs across figures.
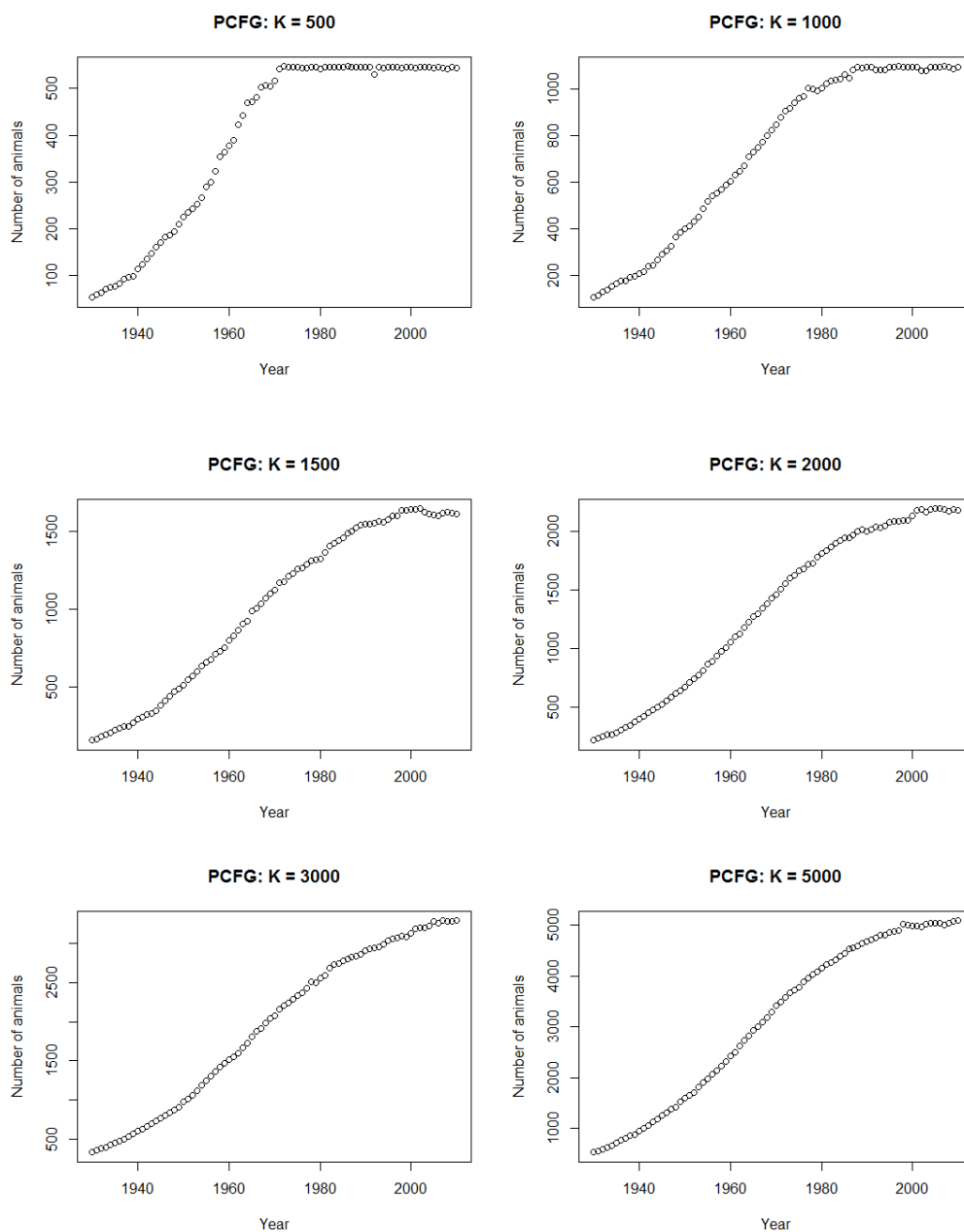
Table 21. Median PCFG abundance in 2010 for scenarios with K_{PCFG} set between 500 and 5000.

K_{PCFG}	N_{2010} (median and 90% range)
500	501 (466 – 542)
1000	998 (923-1063)
1500	1496 (1391-1588)
2000	1994(1864-2080)
3000	3002(2831-3128)
5000	4945 (4790-5095)

Table 22. The expected number of immigrants/year at the cross-over point under the scenarios with and without pulse immigration. The cross-over is derived by calculating the point at which 50% of the simulation replicates produce values for each summary statistic that are higher than that for the empirical data.

Matrices	Timing of split	Pulse migration	Number of haplotypes	Haplotypic diversity	F_{ST}	ϕ_{ST}	χ^2/df
9-stage	Post-whaling split	Y	3.77	7.82	3.84	1.67	3.76
9-stage	Post-whaling split	N	4.35	10.25	4.25	2.11	4.47
5-stage	Post-whaling split	Y	6.76	-----	3.39	1.37	3.39

Appendix:

This appendix includes additional tables and figures aimed at understanding how well the model underlying our simulations is mimicking reality and/or the IR trial structure.

Table A1. Generation time estimates as calculated using different maximum ages for both 5-stage TOSSM and 9-stage matrices.

| | 5-stage matrices | | 9-stage matrices | |
Max Age	K	ZPD	K	ZPD
40	19.52	16.92	21.05	20.59
50	21.68	18.74	23.65	23.86
100	26.04	22.25	28.29	32.87
150	26.64	22.69	28.61	34.93
1000	26.71	22.74	28.63	35.27

Table A2. The number of calves produced per year in simulated datasets at K as compared to data derived from photo-identification studies
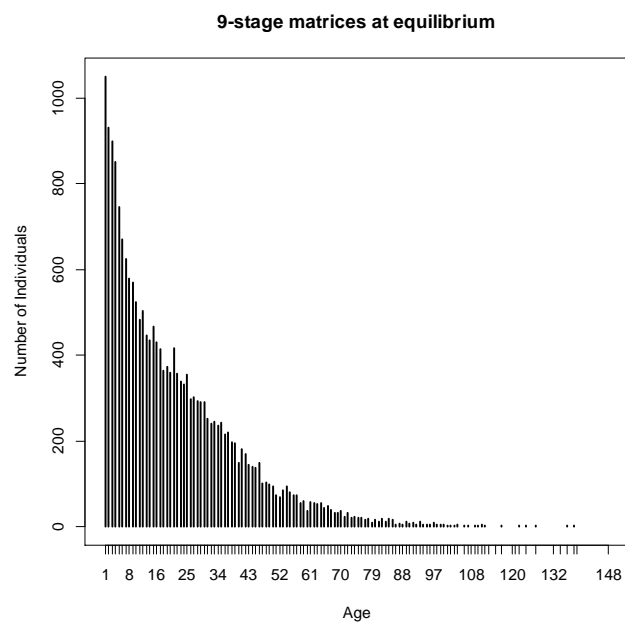
Source	Abundance (median with range):	Number of calves/yr	% Calves
5-stage matrices:	197(156-218)	11 (2-31)	6%
9-stage matrices:	195 (161-217)	10 (2-23)	5%
Photo-identification estimates	194 [†]	3 (0-9)[††]	2%

†Annex F, IWC 2011

†† Calambokidis *et al.* 2008 (data from 1998-2008)

Figure A1. Age distribution in simulated datasets (note different x-axis scales):

a) Nine-stage matrices:

9-stage matrices at equilibrium

a.) Five-stage matrices:

5-stage matrices at equilibrium